COMBUSTION SCIENCE AND TECHNOLOGY
https://doi.org/10.1080/00102202.2023.2170750

Taylor & Francis
Taylor & Francis Group

Cenosphere Formation and Combustion Characteristics of Single Droplets of Vacuum Residual Oils

Hendrix Yulis Setyawan [a] and Mingming Zhu [b]

[a]Department of Agroindustrial Technology, Faculty of Agriculture Technology, Universitas Brawijaya, Malang, East Java, Indonesia; [b]School of Water, Energy and Environment, Cranfield University, Cranfield, Bedfordshire, UK

ABSTRACT

The ignition, combustion characteristics, and cenosphere formation of single droplets combustion of four vacuum residues (VRs) from different refineries with various asphaltene contents were studied experimentally. The single droplets of VRs were suspended at the tip of a silicon carbide fiber and heated in air at temperatures of 973 and 1023 K, respectively, in an electrically heated tube furnace. The ignition and combustion behavior of the VRs were recorded using a CCD camera, which enabled the determination of droplet size, ignition delay time, flame duration, and cenosphere size. The effect of initial droplet size, gas temperature, and asphaltene content on the ignition delay time, flame duration, cenosphere morphology, and particle size were investigated. The whole ignition and combustion process of single droplets of the VRs consisted of five stages in succession: (1) preignition, mainly involving the evaporation of highly volatile components from the droplet surface; (2) steady combustion of fuel vapors evaporated from the droplet surface; (3) splashing combustion of fuel vapors evaporated from droplet interior; (4) disruptive combustion due to thermal decomposition of asphaltene; and (5) solid residue ignition and combustion. A visible and sooty flame was formed upon ignition and lasted during stages 2–4. The droplet size increased sharply in the stage 4 due to the thermal decomposition of asphaltene, which was more profound for VRs with higher asphaltene content and at higher gas temperatures. The ignition delay time increased with increasing initial droplet size and gas temperature but varied little as the asphaltene content in the VRs increased, suggesting that the ignition process of VRs was controlled by the vaporization of high volatile components on the droplet surface. The thermal decomposition of asphaltene produced solid residue, which was in the form of a cenosphere with the shell thickness being ca. 20 μm and a number of blowholes presented in the shell. The VRs with higher asphaltene content had more and bigger blowholes. The ratio of cenosphere particle size to initial droplet size is independent of the initial droplet size but almost increased linearly with the asphaltene content in the VRs.

ARTICLE HISTORY
Received 1 October 2022
Revised 20 December 2022
Accepted 17 January 2023

KEYWORDS
Combustion; cenosphere; droplets; ignition; vacuum residue

CONTACT Mingming Zhu mingming.zhu.152@cranfield.ac.uk School of Water, Energy and Environment, Cranfield University, Cranfield, Bedfordshire MK43 0AL, UK

Introduction

Vacuum residue (VR) is produced as the bottom product from the vacuum distillation unit in a refinery (Ancheyta and Speight 2007). VR can be used as fuel in boilers and industrial furnaces for the heat and/or power generation (Urban and Dryer 1990; Urban, Huey, and Dryer 1992). In utilizing VR as a fuel, the asphaltene, mainly composed of large condensed aromatic hydrocarbons and long paraffinic side chains, contained in the VR is the most problematic as it makes VR extremely viscous and the combustion of asphaltene contributed to the formation of coke, resulting in low combustion efficiency and high unburned carbon emission (Urban and Dryer 1990; Urban, Huey, and Dryer 1992; Xu et al. 2003).

Previous studies (Ikegami et al. 2003; Jiang et al. 2019; Kobayasi 1955; Xu et al. 2002) on heavy fuel oils (HFO) have suggested that the entire combustion process of a heavy oil droplet can be broadly divided into liquid-phase combustion and solid coke combustion, where the liquid phase can be further subdivided into inner evaporation, thermal decomposition, and polymerization toward coke formation. A similar division for the combustion process of heavy oils was also adapted for numerically formulating the evaporation and pyrolysis of heavy oil droplets (Baert 1993). Recently, Villasenor and Garcia (1999) found that the combustion of single droplets of two Mexico-heavy oils with high asphaltene content showed disruptive behavior, characterized by the significant expansion of droplet diameter just before the droplet collapsed to produce a coke particle. The particles either had a porous or a skeleton/membrane morphology (Elbaz, Khateeb, and Roberts 2018). The authors believed that the disruptive combustion was caused by the thermal decomposition of asphaltene, and this phenomenon should be more profound when the asphaltene content was higher. The thermal history of the particle also has a significant impact on the decomposition of asphaltene and therefore the formation of coke (Elbaz, Khateeb, and Roberts 2018). However, this claim was lack of sufficient experimental evidence. Thus, it is necessary to further study the effect of asphaltene content on the ignition and combustion processes of VRs that feature extremely high asphaltene content.

Different from the combustion of light oils such as diesel and kerosene, the combustion of VRs produces coke or cenosphere particles mainly produced from asphaltene, which has adverse impacts on boiler and utility operation (Ancheyta and Speight 2007; Marrone, Kennedy, and Dryer 1984; Xu et al. 2003). One important parameter quantifying the characteristics of cenosphere formation is the particle size (Jiang et al. 2019; Urban and Dryer 1990; Urban, Huey, and Dryer 1992; Xu et al. 2003). It has been reported that the size of a cenosphere particle proportionally varies with the initial droplet size (d_0) following d_0^n. However, discrepancies existed in the literature regarding the value of n. Some found that the value of n equaled one (Kwack et al. 1992), indicating that the volumetric ratio of cenosphere particle to initial droplet size was independent of the initial droplet diameter, while others found that the value of n was bigger than one (Masdin and Thring 1962; Xu et al. 2003), showing that the size ratio of cenosphere particle to initial droplet size proportionally varying with the initial droplet diameter. On the other hand, it was reported that the size ratio of cenosphere particle to initial droplet size linearly correlated with the asphaltene content in the heavy oils (Kwack et al. 1992), but some researchers claimed that the formation of the cenosphere was only dependent on the asphaltene chemical structures while irrespective of the total amount of asphaltene in the fuel (Bomo et al. 1984). Recent findings suggest that over the course of burning, micro-explosive behavior occurred, and

the droplet's maximum size increased due to the higher asphaltene content (Khateeb et al. 2018).

In the present work, experiments on suspended droplets of VRs were carried out in an effort to gain fundamental insights into the ignition and combustion characteristics and cenosphere formation of VRs with various asphaltene contents. Single droplet experimentation was adopted as it has been widely used to study the fundamentals of ignition and combustion of liquid fuels (Aggarwal 2014; Baert 1993; Ikegami et al. 2003; Urban and Dryer 1990; Urban, Huey, and Dryer 1992; Xu et al. 2002, 2003; Zhu et al. 2015; Zhu, Ma, and Zhang 2013). The ignition delay time, flame duration, cenosphere morphology, and particle size as a function of initial droplet size and ambient gas temperature were investigated. The effect of the asphaltene content on morphology, the size of cenosphere particles, and the ratio of cenosphere particle size to the initial droplet size were also investigated. The results will have some practical implications in the design of boilers fueled with VRs and the control of cenosphere emission from the combustion of VRs.

Experimental

Four VRs from different refineries with different asphaltene content were used in the current study, which are Lower Zakum vacuum residue (LZ), Chinese Liaohe vacuum residue (LH), Arab Medium vacuum residue (AM), and Venezuela vacuum residue (VZ). Some salient properties of the four VRs are listed in Table 1.

Single droplet combustion experiments of VRs were carried out using an experimental setup, as shown in Figure 1 (Zhu et al. 2015). Briefly, the experimental rig consisted of a horizontal tube furnace (600 mm in length and 40 mm in diameter) with temperature control for providing a hot air environment, a droplet suspension system, a step motor for delivering the droplet into the furnace and a CCD camera for determining combustion characteristics. In a typical experiment, the tube furnace was heated to the set temperature, in which a VR droplet was ignited and combusted. The droplet was suspended on the tip of a silicon carbide fiber of 142 μm in diameter using a quartz rod. The actual shape of the suspended droplet in the present experimentation was elliptical and a stated droplet size referred to a sphere-equivalent value determined as the cubic root of the product of the droplet width squared and the droplet length (Zhu et al. 2015). A high-speed CCD camera (Basler PIA-210gc) with 200 frames per second was used to capture the images of the entire process from the moment when the droplet entered the furnace until it burned out. To determine the changing droplet size during combustion, the burning droplet was backlit with a 50-W halogen lamp while being recorded on a CCD camera. A computer was used to

Table 1. Some key properties of the four VRs.

Sample Properties	LZ	LH	AM	VZ
Density (gml^{-1}@288K)	0.99	1.01	1.04	1.05
Asphaltene (wt%)	1.05	5.61	7.67	14.58
Conradson carbon residue (wt%)	14.5	18.11	21.5	26.19
Vanadium (ppm)	5.51	3.5	129	751.7
Nickel (ppm)	4.77	155.0	43	175.5
Sulphur (wt%)	3.09	0.50	5.44	4.80
Nitrogen (ppm)	2020	1510	3770	1090

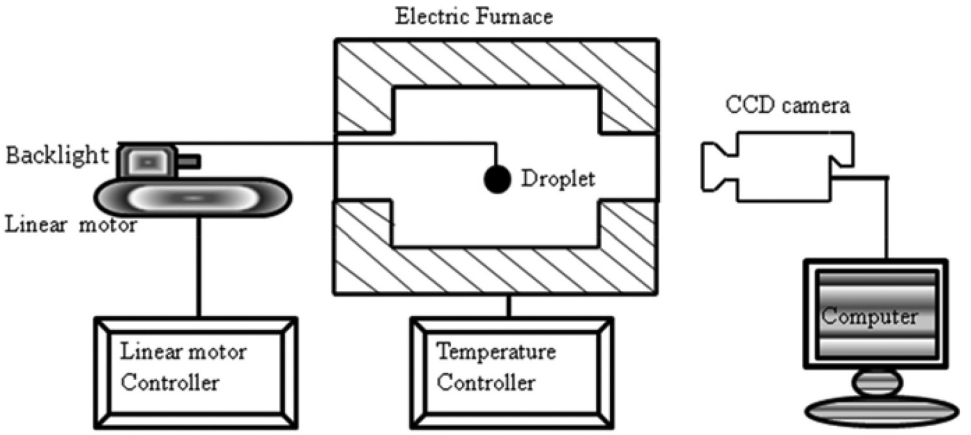

Figure 1. A schematic diagram of the apparatus for experimentation of single droplet combustion.

operate the step motor and the CCD camera. In the present study, the initial droplet diameter varied from 0.5 to 1.0 mm, and the furnace temperatures were fixed at 973 and 1023 K, respectively. Using the optical images taken by the CCD camera, the ignition delay period and flame duration of the burning droplet were determined. The ignition was said to take place when the first visible flame appeared. The ignition delay time was defined as the time from the moment the droplet enters the center of the furnace to the moment when ignition occurred. Once ignition occurred, a flame was formed surrounding the droplet. The total time that the visible flame lasted was taken as the flame duration.

Some of the cenosphere particle samples were taken for morphology analysis. At the moment of flame extinction, the formed cenosphere particles were quickly withdrawn from the center of the furnace with the aid of the step motor. The morphology of cenosphere particles collected was analyzed using a Tescan SEM operating at 20kV and magnification at 200× and 500×, respectively.

Results and discussion

Ignition and combustion phenomena of VRs

Typical sequences of images of the ignition and combustion processes of suspended droplets of VZ vacuum residue in the air at a temperature of 1023K with and without backlight are illustrated in Figure 2. The initial droplet diameter was around 1 mm measured prior to experimentation. The variation of the diameter of the backlit burning droplet shown in Figure 2 as a function of heating time was also calculated and presented in Figure 3. From the combustion phenomenon and the change of droplet diameter, the ignition and combustion of the droplets were divided into five stages in succession: (1) **pre-ignition**: when the droplets were exposed to hot air, the droplets were heated and evaporated, and the high volatile components were released. The vaporized components were mixed with ambient air, and when the mixtures reached the ignition condition, the droplets ignited, and a visible flame appeared (No.1 in Figure 2). In this stage, the droplet diameter slightly increased due to the heating and swelling of the droplet (stage 1 in Figure 3); (2)

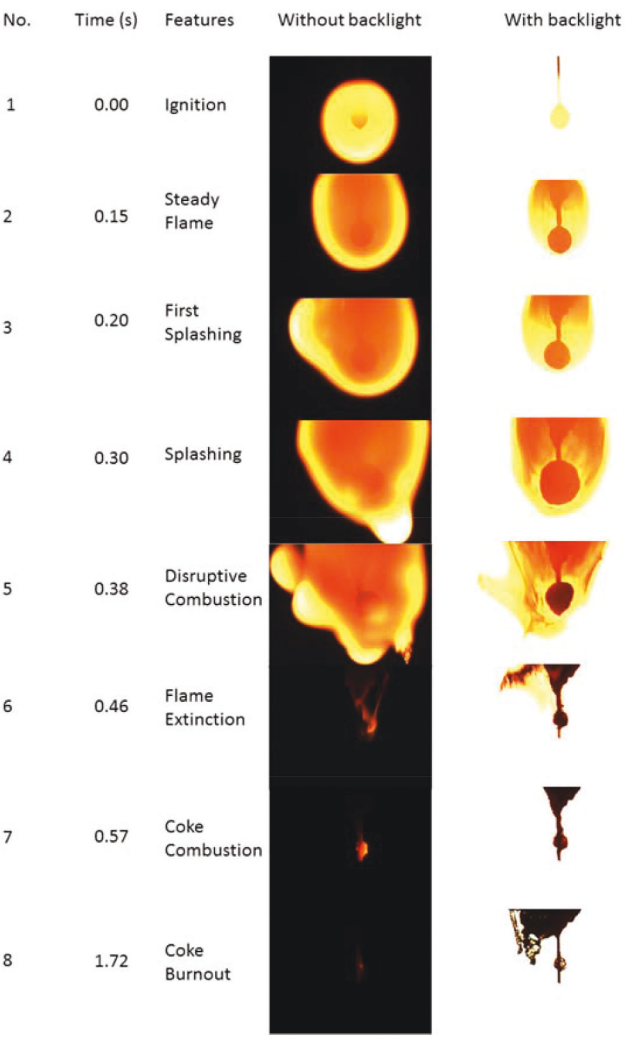

Figure 2. Typical photographic sequences of the ignition and combustion processes of droplets of VZ at 1023K.

steady combustion: after ignition, the droplets burned quiescently for a period, during which the flame was steady without distortion and deformation, and the droplet was also nearly spherical with little surface distortion (No.2 in Figure 2). The droplet diameter experienced a rapid increase after ignition (stage 2 in Figure 3). This sharp increase in diameter was due to enhanced heating from the flame formed. These features indicate that it is most likely that vaporization of the fuel occurred on the droplet surface during this steady combustion phase as both the droplet and the flame remained uninterrupted; (3) **splashing combustion**: The steady flame lasted ca.0.2s until it experienced the spark-like flashes (No.3 in Figure 3). The flash, also known as splashing, represented weak puffs of fuel vapors from the droplet surface (Kwack et al. 1992). In this combustion period (Nos. 3 and 4 in Figure 2), the flame size increased considerably, and the flame shape was slightly distorted caused by the ejection of a few small fuel satellites from the droplet through the flame front. The shape

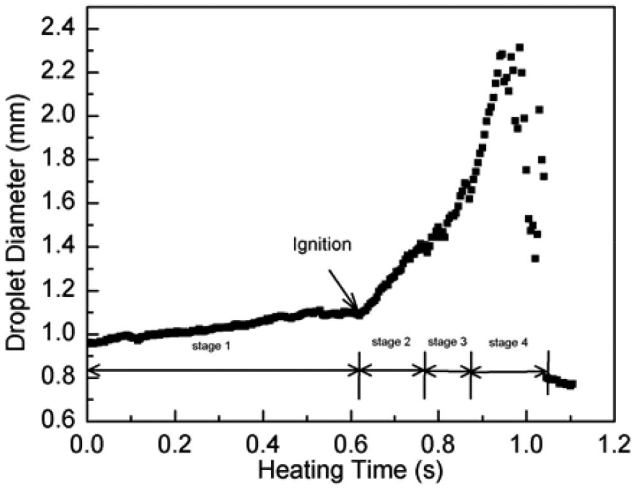

Figure 3. Diameter variation of the backlit droplet of VZ shown in Figure 2 as a function of heating time at 1023K.

of the droplet became slightly irregular. The droplet swelling generally made the droplet foam-like with small bubbles observed inside the droplet. Accordingly, the droplet size continued to increase, but the increase rate was slightly slower than that in stage 2 (stage 3 in Figure 3). The droplet size also fluctuated, indicating the swelling and contraction of the droplet. These features suggest that the evaporation of fuel inside the droplet occurred. As the burning progressed into the splashing combustion stage, the heat was transported into the droplet interior and temperature inside the droplet possibly reached the boiling points of some components with high volatility, leading to inner evaporation and the rapid generation of vapor within the droplet (Kwack et al. 1992). The shape of the droplet varied during this period, indicating that the droplet surface was still fluid enough with relatively low viscosity that could allow the vapors generated inside the droplet to pass through the droplet surface. As a result, some of the fuels ejected from the droplet surface, distorting both the droplet and flame and leading to the swelling and contraction of the droplet; (4) **disruptive combustion**: as the combustion progressed, at 0.38s (No.5 in Figure 2), the droplet exploded and the combustion became disruptive, leading to the considerable deformation of the flame and micro-explosion of the droplet. It was also observed that a number of bubbles formed and grew inside the droplet. Accordingly, when the combustion changed from the splashing into the disruptive combustion stage, the droplet diameter increased sharply again and reached a maximum value shortly (stage 4 in Figure 3), after which the droplet micro-exploded, leading to the droplet collapse. It is believed the disruptive combustion was caused by the thermal decomposition of heavy components known as asphaltene. The thermal decomposition produced a large amount of gases, which swell the droplet, leading to a sharp increase in the droplet. Since the droplet surface became more viscous after the evaporation of highly volatile components in previous combustion stages, the gas trapped inside the droplet could not escape from the droplet easily, leading to an expanse of the droplet size and the pressure buildup inside the droplet. When the pressure buildup was high enough, the droplet exploded and the flame deformed; and (5) **solid residue ignition and combustion**: After thermal decomposition, the droplet

condensed and transformed into solid particles deposited on the tip of the fiber (No.6 in Figure 2). Upon the flame extinction, the coke particles ignited and burned (No.7 in Figure 2) until the end of the combustion (No.8 in Figure 2).

Soot was also formed during the combustion stages 2–4. Figure 2 shows that the soot was likely to form in the vicinity of the droplet, causing an obvious soot cloud surrounding the droplet. In the combustion stages 3 and 4, the soot particles tended to move upward because of the buoyancy effect and finally agglomerated and lumped and deposited on the surface of the fiber.

The overall ignition and combustion characteristics of the four VRs are similar as described above but VRs with higher asphaltene content showed a higher degree of disruptive combustion in combustion stage 4 as mentioned above, confirming that it is the decomposition of asphaltene that caused the disruptive combustion in this stage.

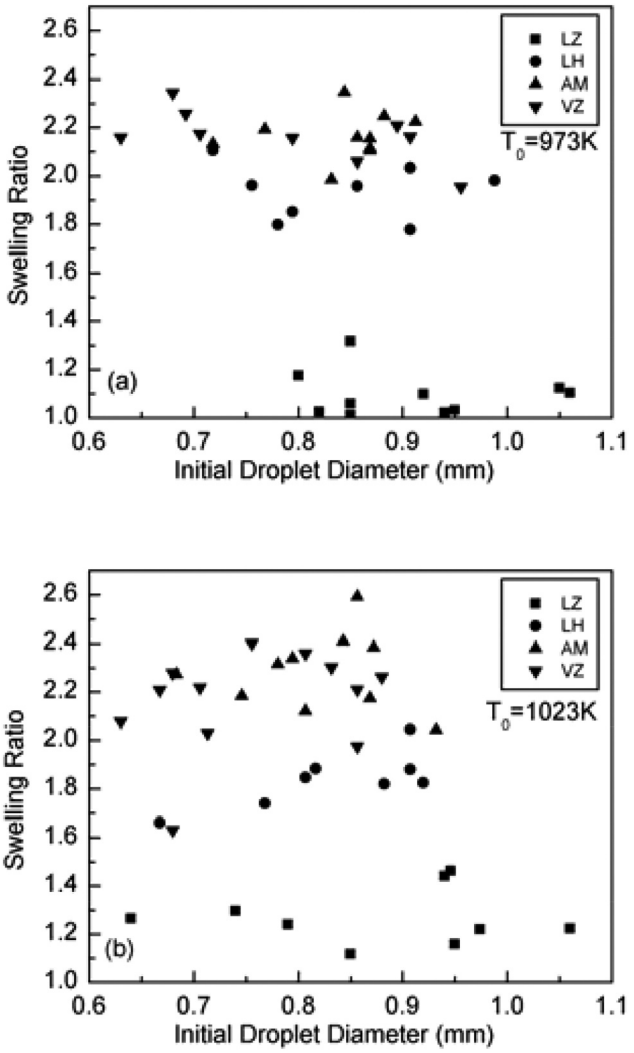

Figure 4. Swelling ratios of single droplets of the VRs against initial droplet size.

Figure 4 shows the swelling ratio of the droplets against the initial droplet size for the four VRs at different gas temperatures, respectively. The swelling ratio was defined as the ratio of the maximum droplet size during swelling to the initial droplet size. It is evident that, for a given VR, the swelling ratio remained constant regardless of the initial droplet size under the tested conditions. This suggests that the maximum droplet size increased nearly linearly with the initial droplet diameter. As can be seen in Figure 4, for VRs with higher asphaltene content, the swelling ratio was bigger. This confirms the previous discussion that the decomposition of asphaltene was responsible for the swelling of the droplet just before the droplet collapsed to form coke. With higher asphaltene content in the VRs, a larger amount of gas was produced during the thermal decomposition process, leading to a stronger swell of the droplet. It was also found that increasing the ambient temperature from 973 to 1023 K slightly increased the swelling ratio of the droplet for any of the four VRs. In principle, a higher ambient temperature leads to a higher flame temperature and higher heating rate transferred to the droplet. It has been found that during the thermal decomposition process, a higher heating rate or ambient temperature normally yielded more gases (Bridgwater 2012). As a consequence, the swelling ratio of the droplet was slightly enhanced at a higher ambient temperature.

Ignition delay time

Figure 5 shows the ignition delay time of the four VRs against the initial droplet diameter at different ambient temperatures. It is observed that the ignition delay times of VRs increased with increasing droplet size and decreasing gas temperature. The ignition delay time of a single droplet is composed of a physical delay during which the droplet evaporates, and the fuel vapor diffuses outwards, and a chemical delay during which the fuel vapor reacts with the oxidant to release heat. Obviously, the ignition of the droplets of VRs was controlled by the vaporization of the fuel (Law 1978) at the tested conditions, as it took more time to heat the droplet up and reach the ignition temperature of the fuel for a bigger droplet.

It is also seen that there are no significant differences among the four VRs in terms of ignition delay time at 973 K, while the ignition delay time of VM was slightly higher than that of the other three VRs at 1023 K. Xu et al. (2002) claimed that the ignition delay time increased with increasing asphaltene content in heavy oils. However, the current study and some of the literature reports (Baert 1993) suggest that there was no direct correlation between the amount of asphaltene and the ignition delay time for VRs from different refineries. The VRs are multicomponent mixtures and the volatility differences of different components are so large that it is most likely that the ignition process of VRs was diffusion-controlled (Lasheras, Fernandez-Pello, and Dryer 1981; Law 1978; Makino and Law 1988; Takei, Tsukamoto, and Niioka 1993; Wang and Law 1985), in which the mass transportation inside the droplet is the limiting step. In the diffusion-controlled ignition process, the more-volatile component from the droplet surface evaporates first and the evaporation is dominated by the more-volatile component in a thin layer at the droplet surface. The surface temperature is relatively low as it is controlled by the boiling point of the more-volatile component. Once the ignition conditions are met, the ignition of more-volatile components occurs. At this stage, the ignition delay time was controlled by the ignition characteristics of the more-volatile matter. If the ignition of more-volatile matter fails, the

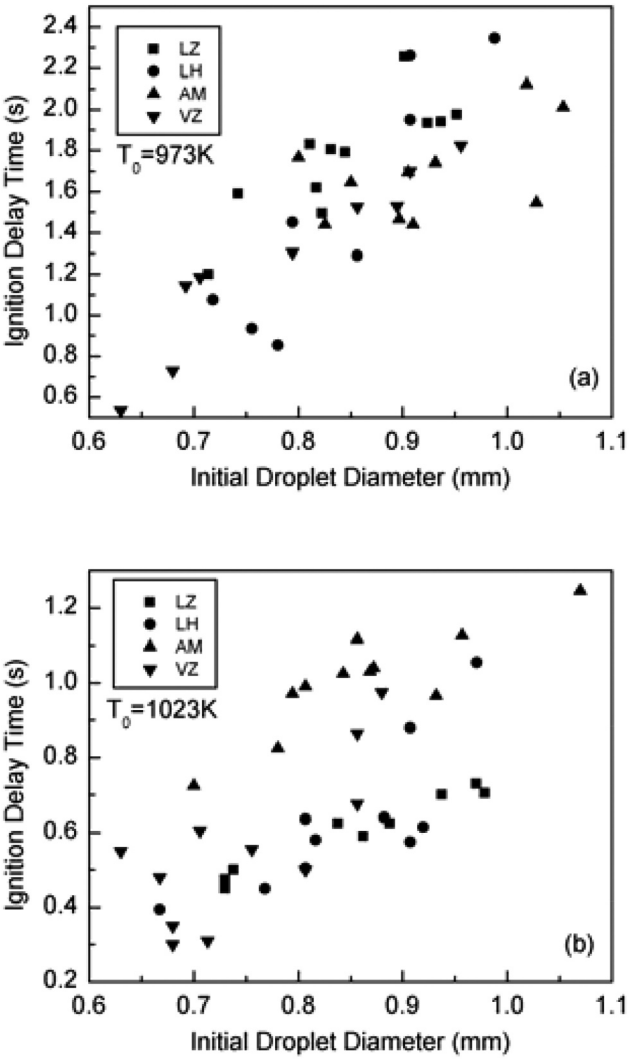

Figure 5. Ignition delay times of the VRs against initial droplet size.

heating up of less-volatile components at the surface will start since more-volatile components cannot be easily transported from the droplet interior to the surface due to slow liquid-phase transport. The surface temperature of the droplet continues to increase to reach the boiling point of the less-volatile components, and the evaporation was controlled by the less-volatile components. The present findings suggest that the ignition of VRs was controlled by the more-volatile matter in the VRs, meaning that the more-volatile components evaporated from the droplet surface reached the ignitable limit before the less-volatile components took a role in the ignition process. The results also indicated that the more-volatile matter that caused the ignition in the four VRs seems to possess similar ignition characteristics, the reason why the ignition delay time varied little for the four VRs at the tested conditions. Both the experimental studies on the ignition delay time of heptane/hexadecane (Khan and Baek 2006) and the detailed mathematical modeling on the ignition

of single heptane/iso-octane droplets (Stauch and Maas 2007) found that when the fraction of more-volatile component, heptane in both cases, was higher than certain values, the ignition delay time varied little by increasing the fraction of high volatile component. If a VR is simply regarded as a bi-component consisting of maltene and asphaltene, the ignition of the VR is most likely controlled by the ignition characteristics of maltene, not asphaltene, when the asphaltene content was not high enough.

Flame duration

The flame durations of the combustion of the four VRs against the initial droplet diameter at different ambient temperatures are presented in Figure 6. It is seen that at both gas temperatures, for all four VRs, the flame duration increased as the droplet size increased.

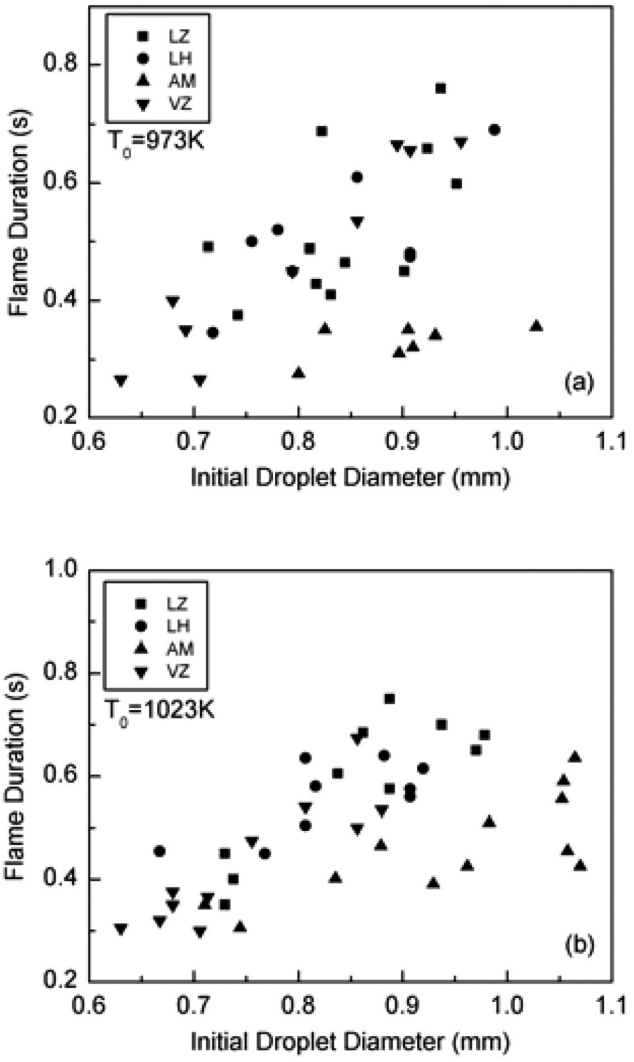

Figure 6. Flame durations of the VRs against initial droplet size.

There was no significant difference in the flame duration among LZ, LH, and VZ but the AM droplets showed much lower flame durations than that of the other three fuels. This is consistent with some of the literature reports that the flame duration was independent of the asphaltene content in the VRs (Xu et al. 2002). As the total amount of fuel vapors could either come from the evaporation of highly volatile components (maltene) or be generated from the decomposition of less volatile components (asphaltene) in VRs, both the properties of the maltene and asphaltene have to be considered to evaluate the flame duration of the VR during the combustion process. Note that the decomposition of asphaltene also resulted in the very strong disruptive and explosive combustion of the droplet, as shown in Figure 2, which would enhance the heat and mass transfer and subsequently improve the reaction rates of fuel vapors in the air. This phenomenon was more significant for VRs with higher asphaltene content, leading to shorter flame durations for VRs with higher asphaltene content.

Cenosphere morphology

Figure 7 (A1-A4) shows the SEM images of the solid particles deposited on the fiber for the four VRs at 1023 K, respectively. In order to obtain detailed morphology information inside the particle, the higher resolution SEM images of the cleaved particles that were peeled off from the fiber are also illustrated in Figure 6 (B1-B4). It is evident that the particles formed were cenospheres, which were hollow inside and composed of hard shells. It is also clear that there were many blowholes present on the shell of the particles. This is consistent with the observations shown in Figure 2 that the bubbles were formed inside the droplet during the combustion process making the droplet foam-like. From the previous discussion, during the combustion of VRs, the fuel vapors from the evaporation of the high volatile components in the droplets in the stage 3 combustion and gases from thermal decomposition of low volatile components in the stage 4 escaped through the shell, leaving solid residues on the fiber in the form of a cenosphere. If the strength of the cenosphere shell is weak, the expelling gas would rupture the viscous shell and produce blowholes. The sizes of the blowholes varied for a given VR, indicating different degrees of disruptive ejections of fuel vapors and gases from the interior of the droplets.

It is also seen that VRs with higher asphaltene content seemed to have more and bigger blowholes. There was no significant difference in the thickness of the shell among the four VRs, which was ca. 20 μm. This is consistent with some of the literature reports on cenosphere morphologies for VRs with different asphaltene contents (Kwack et al. 1992) but different from the experimental results (Xu et al. 2003). By varying the asphaltene content in VRs by blending a VR with a diesel oil at different fractions, Xu et al. (2003) found that higher fractions of diesel in the blends resulted in thicker shells and more blowholes and claimed that the evaporation of diesel mainly contributed to this phenomenon. However, the current results, including both the phenomenological observations of the combustion process of single droplets and the cenosphere morphologies of VRs with various asphaltene contents, revealed that it is the thermal decomposition of low volatile components at the combustion stage 4 of the combustion, rather than the evaporation of highly volatile components in the VRs, that caused the formation of final morphology of the cenosphere and the blowholes on the particles. The higher the asphaltene content in the VR, the more amounts of gaseous hydrocarbons produced from the thermal decomposition of asphaltene,

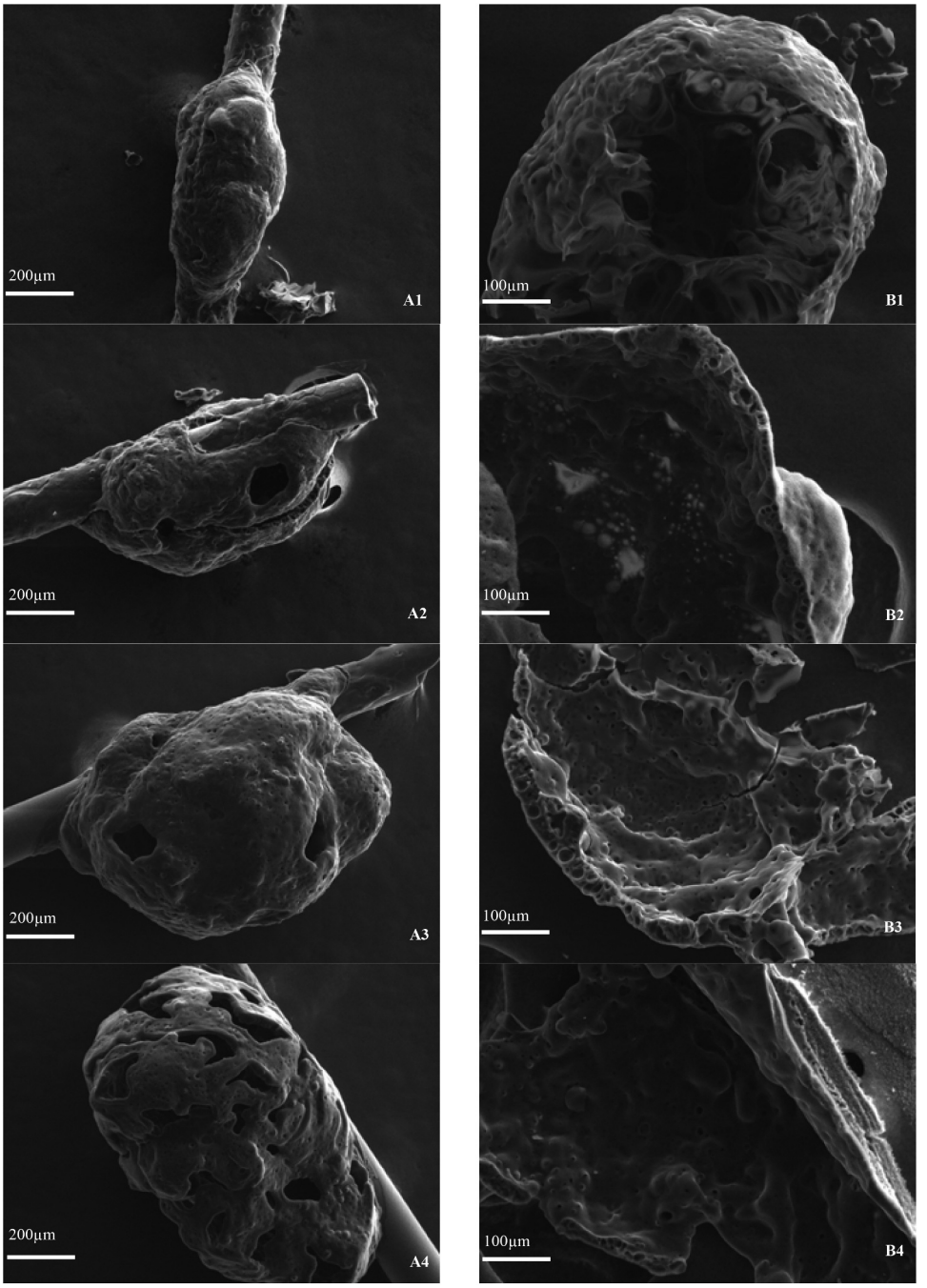

Figure 7. Typical SEM images of coke particles from the four VRs (A: original coke particles attached on the fiber; B: cleaved coke particles peeled from the fiber; 1: LZ; 2: LH; 3: AM; 4: VZ).

leading to higher pressure buildup inside the droplet and stronger ejection and subsequently bigger and more blowholes.

Cenosphere size

Figure 8 illustrates the measured cenosphere particle diameter (D_c) against the initial droplet diameter (D_0) for LH, AM, and VZ at temperatures of 973 and 1023 K, respectively. The size of cenosphere particles from the combustion of LZ has not been included in Figure 8 as the combustion of the LZ residue produced very small cenospheres, making it difficult to accurately measure the size of the cenosphere in the present study. Note that the cenosphere diameter in this study was the effective diameter that excluded the fiber

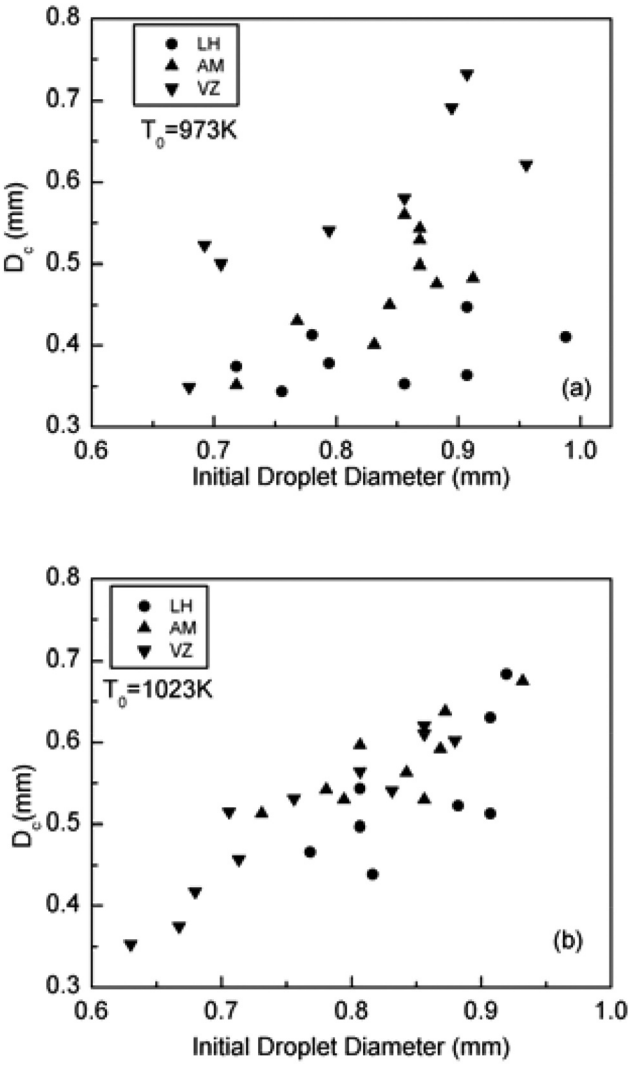

Figure 8. Coke particle sizes as a function of initial droplet diameter for different VRs at different gas temperatures.

diameter using the method used by (Xu et al. 2003). As shown in Figure 7, D_c increased with increasing the initial D_0. At a given D_0, the D_c followed the order of VZ > AM > LH, irrespective of the gas temperature. It seems that the D_c was higher for VR with higher asphaltene content, indicating that the thermal decomposition of asphaltene was the main contributor to the formation of the cenosphere. Increasing gas temperature also slightly increased the cenosphere size, which complies with the previous observation that the droplet swelling ratio was slightly higher at higher gas temperatures.

The ratios of D_c to D_0 at different gas temperatures for the three VRs, respectively, are shown in Figure 9. Clearly, the size ratio was independent of the initial droplet size at the tested conditions. This is consistent with the experimental results reported by Marrone, Kennedy, and Dryer 1984) and Kwack et al. (1992). The burning of a bigger droplet would

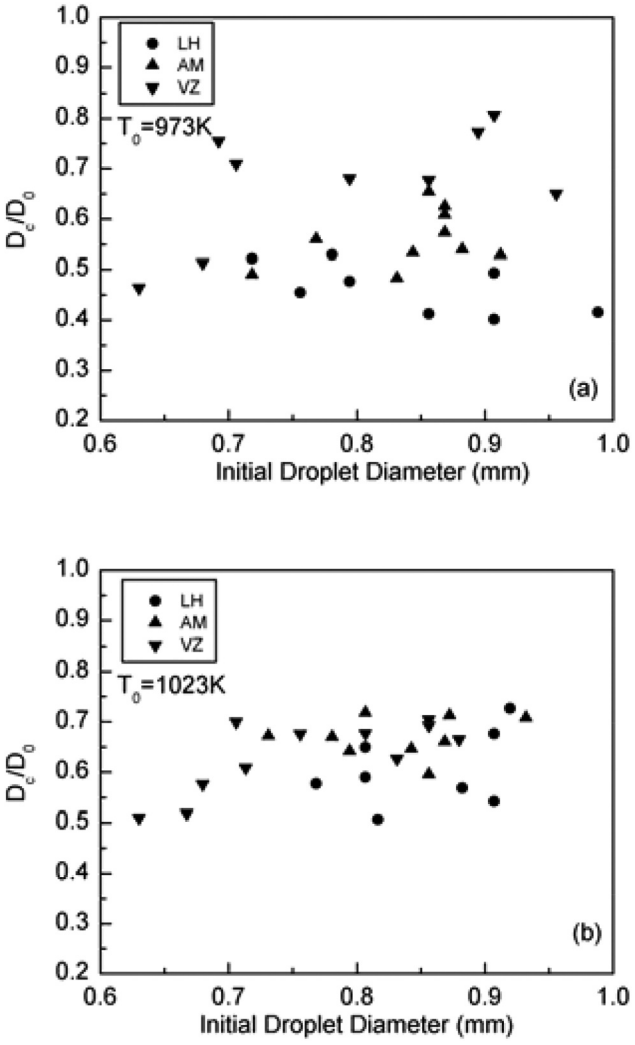

Figure 9. Size ratio of coke particle to initial droplet as a function of initial droplet diameter for different VRs at different gas temperatures.

lead to a larger volume of the cenosphere, which may result from an increased cenosphere mass and/or cenosphere volume expansion. Urban and Dryer (1990) and Urban, Huey, and Dryer (1992) found that the ratio of cenosphere mass to the initial droplet mass was independent of the initial droplet size. The current study has also demonstrated that the droplet swelling ratio was irrespective of the initial droplet size at droplet sizes tested, as shown in Figure 4. Therefore, the ratio of D_c to D_0 had little variation by changing the initial droplet size. It is also seen from Figure 8 that the ratios of D_c to D_0 for the VRs were slightly increased as the gas temperature increased, which may be attributed to the increased droplet swelling ratio at higher gas temperatures, as shown in Figure 4.

Another piece of information obtained from Figure 9 is that the size ratios of D_c to D_0 increased for VRs with higher asphaltene content. The size ratio of D_c to D_0 vs the asphaltene content in the VRs is then plotted in Figure 10. The experimental data from the current study were taken at 1023 K. This would not change the overall trend shown in Figure 10, as the gas temperature only showed a small effect on the size ratio, as discussed above. The data from the literature (Urban and Dryer 1990; Urban, Huey, and Dryer 1992; Xu et al. 2003) were also included in Figure 9 for a comparison. Pei, Tian, and Roberts (2022) showed that increasing asphaltene content increased the cenosphere size due to the difficulty of burning asphaltenes, which are heavy polycyclic aromatic compounds with embedded heteroatoms. Large light-weight and hollow cenospheres were produced during the inefficient combustion process (Pei, Tian, and Roberts 2022). Kwack et al. (1992) suggested that the size ratio linearly increased with the asphaltene content in the VRs, but the VRs used in their experiments had relatively low asphaltene content (less than 10%). It is seen from Figure 10 that such a linear correlation is still valid when the asphaltene was as high as ca. 20%. The current findings have some significant practical implications for VRs that the asphaltene content can be used as an indicator for predicting the size of coke particles, regardless of the chemical structures of the asphaltene. Reducing the cenosphere size can be effectively achieved by suppressing the asphaltene content in the fuel, such as by adding water into the fuel or diluting the heavy oil with light oils (Goldstein and Siegmund 1976; Ocampo-Barrera, Villasenor, and Diego-Marin 2001).

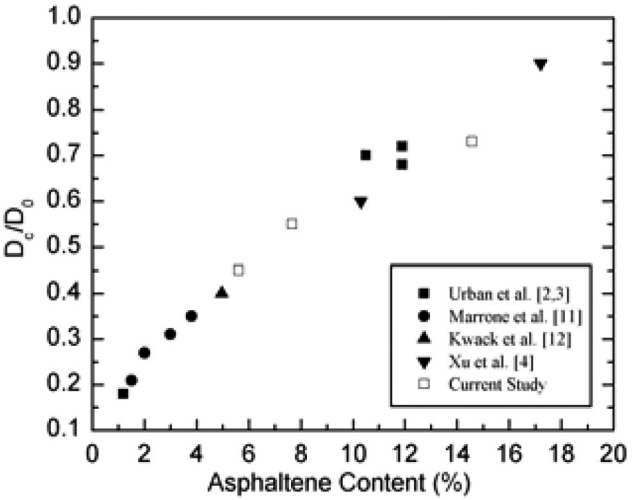

Figure 10. Effect of asphaltene content in VRs on the size ratio of coke particle to initial droplet.

Conclusions

The ignition and combustion characteristics and cenosphere formation of suspended single droplets of four VRs from different refineries with various asphaltene contents were studied. The effect of initial droplet size and gas temperature on the ignition delay time, flame duration, cenosphere morphology, and particle size was investigated. The following conclusions can be drawn:

- The whole ignition and combustion process of single droplets VRs included five stages in succession: (1) pre-ignition, mainly involving the evaporation of highly volatile components from the droplet surface; (2) steady combustion of fuel vapors evaporated from the droplet surface; (3) splashing combustion of fuel vapors evaporated from droplet interior; (4) disruptive combustion due to thermal decomposition of the low volatile component; and (5) solid ignition and combustion to form cenospheres. A visible and sooty flame was formed upon ignition and lasted during stages 3 and 4.
- Thermal decomposition of asphaltene resulted in the significant swelling of the droplet size, which was more profound for VRs with higher asphaltene content and at higher gas temperatures. The ignition delay time increased with increasing the initial droplet size and gas temperature, but varied little as the asphaltene content in the VRs increased, suggesting that the ignition process of VRs was diffusion-controlled and dominated by the vaporization of high volatile components on the droplet surface.
- The thermal decomposition of asphaltene produced coke, which was in the form of a cenosphere with the thickness of the shell being ca. 20 μm and a number of blowholes in the shell. VRs with higher asphaltene content had more and bigger blowholes. The cenosphere particle size almost increased linearly with the initial droplet size and increasing gas temperature slightly increased the coke particle size.
- The present results also suggest that the asphaltene content can be used as an indicator of the size of the cenosphere particles without knowing the chemical structures of the asphaltene as the ratio of the cenosphere particle to the initial droplet size almost linearly increased with the asphaltene content in the VRs.

Highlights

- Ignition and combustion process of VRs consisted of five successive stages
- Ignition process was controlled by the evaporation of fuels on the droplet surface
- Thermal decomposition of asphaltene resulted in coke in the form of cenosphere
- Cenosphere particle size increased linearly with initial droplet size
- Cenosphere particle size increased linearly with asphaltene content in VRs

Acknowledgement

The authors would like to acknowledge the support of the Centre for Biomass Research at Universitas Brawijaya.

Disclosure statement

No potential conflict of interest was reported by the authors.

ORCID

Hendrix Yulis Setyawan http://orcid.org/0000-0002-3513-977X
Mingming Zhu http://orcid.org/0000-0002-3643-1799

References

Aggarwal, S. K. 2014. Single droplet ignition: Theoretical analyses and experimental findings. *Prog. Energy Combust. Sci.* 45:79–107. doi:10.1016/j.pecs.2014.05.002.

Ancheyta, J., and J. G. Speight. 2007. *Hydroprocessing of heavy oils and residue*. Boca Raton: CRC Press. doi:10.1201/9781420007435.

Baert, R. S. G. 1993. A mathematical model for heavy fuel droplet vaporisation and pyrolysis in a high temperature inert gas. *Combust. Sci. Technol.* 90 (1–4):125–47. doi:10.1080/00102209308907607.

Bomo, N., J. Lahaye, G. Prado, and G. Claus. 1984. Formation of cenosphere during pyrolysis of residual fuel oils. *Symp. (Int.) Combust.* 20 (1):903–11. doi:10.1016/S0082-0784(85)80579-8.

Bridgwater, A. V. 2012. Review of fast pyrolysis of biomass and product upgrading. *Biomass Bioenergy.* 38:68–94. doi:10.1016/j.biombioe.2011.01.048.

Elbaz, A. M., A. A. Khateeb, and W. L. Roberts. 2018. PM from the combustion of heavy fuel oils. *Energy* 152:455–65. doi:10.1016/j.energy.2018.03.163.

Goldstein, H. L., and C. W. Siegmund. 1976. Influence of heavy fuel oil composition and boiler combustion conditions on particulate emissions. *Environ. Sci. Technol.* 10:1109–14. doi:10.1021/es60122a006.

Ikegami, M., G. Xu, K. Ikeda, S. Honma, H. Nagaishi, D. L. Dietrich, and Y. Takeshita. 2003. Distinctive combustion stages of single heavy oil droplet under microgravity. *Fuel* 82:293–304. doi:10.1016/S0016-2361(02)00257-0.

Jiang, L., A. M. Elbaz, P. Guida, S. Al-Noman, I. A. ALGhamdi, S. Saxena, and W. L. Roberts. 2019. Cenosphere formation during single-droplet combustion of heavy fuel oil. *Energy Fuels.* 33 (2):1570–81. doi:10.1021/acs.energyfuels.8b03632.

Khan, Q. S., and S. W. Baek 2006, Effects of high ambient pressure and temperature on the autoignition of blended fuel droplets, *International Conference on Energy and Environment*. Bangi, Selangor, Malaysia, 56–60.

Khateeb, A. A., A. M. Elbaz, P. Guida, and W. L. Roberts. 2018. Influence of asphaltene concentration on the combustion of a heavy fuel oil droplet. *Energy Fuels.* 32 (12):12981–91. doi:10.1021/acs.energyfuels.8b03260.

Kobayasi, K. 1955. An experimental study on the combustion of a fuel droplet. *Symp. (Int.) Combust.* 5:141–48. doi:10.1016/S0082-0784(55)80021-5.

Kwack, E. Y., P. Shakkottai, P. F. Massier, and L. H. Back. 1992. Morphology of globules and cenospheres in heavy fuel oil burner experiments. *J. Eng. Gas Turbines Power* 114:338–45. doi:10.1115/1.2906594.

Lasheras, J. C., A. C. Fernandez-Pello, and F. L. Dryer. 1981. On the disruptive burning of free droplets of alcohol/n-paraffin solutions and emulsions. *Symp. (Int.) Combust.* 18 (1):293–305. doi:10.1016/S0082-0784(81)80035-5.

Law, C. K. 1978. Internal boiling and superheating in vaporizing multicomponent droplet. *AIChE J.* 24 (4):626–32. doi:10.1002/aic.690240410.

Makino, A., and C. K. Law. 1988. On the controlling parameter in the gasification behavior of multicomponent droplets. *Combust. Flame* 73:331–36. doi:10.1016/0010-2180(88)90027-2.

Marrone, N. J., I. M. Kennedy, and F. L. Dryer. 1984. Coke formation in the combustion of isolated heavy oil droplets. *Combust. Sci. Technol.* 36 (3–4):149–70. doi:10.1080/00102208408923731.

Masdin, E. G., and M. W. Thring. 1962. Combustion of single droplets of liquid fuel. *J. Inst. Fuel* 35:251–60.

Ocampo-Barrera, R., R. Villasenor, and A. Diego-Marin. 2001. An experimental study of the effect of water content on combustion of heavy fuel oil/water emulsion droplets. *Combust. Flame* 126 (4):1845–55. doi:10.1016/S0010-2180(01)00295-4.

Pei, X., H. Tian, and W. L. Roberts. 2022. Swirling flame combustion of heavy fuel oil blended with diesel: Effect of asphaltene concentration. *Energies* 15 (17):6156. doi:10.3390/en15176156.

Stauch, R., and U. Maas. 2007. The auto-ignition of single *n*-heptane/*iso*-octane droplets. *Int. J. Heat Mass Transf* 50 (15–16):3047–53. doi:10.1016/j.ijheatmasstransfer.2006.12.005.

Takei, M., T. Tsukamoto, and T. Niioka. 1993. Ignition of blended-fuel droplet in high-temperature atmosphere. *Combust. Flame* 93 (1–2):149–56. doi:10.1016/0010-2180(93)90089-L.

Urban, D. L., and F. L. Dryer. 1990. New results on coke formation in the combustion of heavy-fuel droplets. *Symp. (Int.) Combust.* 23 (1):1437–43. doi:10.1016/S0082-0784(06)80411-X.

Urban, D. L., P. C. Huey, and F. L. Dryer. 1992. Evaluation of the coke formation potential of residual fuel oils. *Symp. (Int.) Combust.* 24 (1):1357–64. doi:10.1016/S0082-0784(06)80158-X.

Villasenor, R., and F. Garcia. 1999. An experimental study of the effects of asphaltenes on heavy oil droplet combustion. *Fuel* 78 (8):933–44. doi:10.1016/S0016-2361(99)00010-1.

Wang, C. H., and C. K. Law. 1985. Microexplosion of fuel droplets under high pressure. *Combust. Flame* 59 (1):53–62. doi:10.1016/0010-2180(85)90057-4.

Xu, G., M. Ikegami, S. Honma, K. Ikeda, X. X. Mao, and H. Nagaishi. 2003. Burning droplets of heavy oil residual blended with diesel light oil: Analysis of coke behaviors. *Energy Fuels.* 17 (3):779–90. doi:10.1021/ef020197b.

Xu, G., M. Ikegami, S. Honma, K. Ikeda, H. Nagaishi, and Y. Takeshita. 2002. Burning droplets of heavy oil residual blended with diesel light oil: Characterisation of burning steps. *Combust. Sci. Technol.* 174 (2):115–45. doi:10.1080/714922711.

Zhu, M. M., Y. Ma, and D. K. Zhang. 2013. Effect of a homogeneous combustion catalyst on combustion characteristics of single droplets of diesel and biodiesel. *Proc. Combust. Inst* 34 (1):1537–44. doi:10.1016/j.proci.2012.06.055.

Zhu, M. M., Y. Ma, Z. Z. Zhang, Y. L. Chan, and D. K. Zhang. 2015. Effect of oxygenates addition on the flame characteristics and soot formation during combustion of single droplets of a petroleum diesel in air. *Fuel* 150:88–95. doi:10.1016/j.fuel.2015.02.009.